Numerical Investigation of the Schrödinger Equation

TFY4235 - Assignment 2

Sami Laubo

March 13, 2024

***Abstract*—*This report investigates quantum mechanical simulations and theory for a particle in three different box potentials. For the method of expanding the wave function in the basis of the eigenstates, it is observed that while the error in eigenvalues increases accordingly with increasing quantum number, the method yields satisfactory results for initial states characterized by smooth functions, albeit encountering numerical instabilities with functions possessing steep slopes or discontinuities. Introducing a potential barrier within the system results in symmetric eigenstate "pairs" with closely spaced eigenvalues, for states with eigenvalues less than the potential barrier strength. The quantum phenomena of tunneling is also observed for this potential. The forward Euler and Crank-Nicolson step-by-step method were also investigated, and it was found that they greatly depend on the dicretization parameters to not exhibit numerical instabilities. The Crank-Nicolson method outperforms the expansion method for discontinuous initial functions. Further insights into eigenvalues and tunneling amplitudes were gained from a two-level detuned system.*

1. Introduction

Quantum physics describes the behavior of particles at the smallest scales, often defying classical intuition. One such scenario is a particle confined in a finite region in a box potential. This seemingly simple case includes many of the foundational concepts in quantum physics. This report seeks to investigate the Schrödinger equation for a particle in a box to analyse the systems behaviour. Through both theoretical and numerical analysis different potentials are explored, where amongst other quantum tunneling occur. The numerical stability and correctness of different numerical approaches are also analysed.

2. Theory and method

2.1. Particle in a box

A particle in the world of quantum mechanics is modelled by the wave function Ψ and its evolution is described by the Schrödinger equation,

$$i\hbar\frac{\partial}{\partial t}\Psi = \hat{H}\Psi. \tag{1}$$

Given the Hamiltonian operator $\hat{H}$ of a system, Eq. (1) describes how the particle evolves in space and time. The Hamiltonian is the part that describes the system and can be hard to find in complicated cases, but in the simple case of a single particle with mass m in a one dimensional box with potential

$$V(x) = \begin{cases} 0, & \text{for } 0 < x < L \\ \infty, & \text{otherwise,} \end{cases} \tag{2}$$

the Hamiltonian reads

$$\hat{H} = -\frac{\hbar^2}{2m}\frac{\partial^2}{\partial x^2} + V(x), \tag{3}$$

where the potential term is zero when considering a particle confined inside the box. Since this Hamiltonian is time-independent, Eq. (1) has the solution

$$\Psi = exp\left(-\frac{it}{\hbar}\hat{H}\right)\Psi_0, \tag{4}$$

where $\Psi_0 = \Psi(x, t = 0)$ is the given initial condition. We thus have an equation that describes the evolution of the wave function. However, to fully utilize this solution we need to know the eigenfunctions of the Hamiltonian, which provide a complete basis for expanding any wave function in this system. These eigenfunctions can be obtained by solving the time-independent Schrödinger equation

$$\hat{H}\psi_n = E_n\psi_n. \tag{5}$$

The eigenfunctions ψ_n in Eq. (5) are called eigenstates and have corresponding energy E_n. Using our Hamiltonian in Eq. (3), the time-dependent Schrödinger equation (1) becomes

$$-\frac{\hbar^2}{2m}\frac{\partial^2}{\partial x^2}\Psi = i\hbar\frac{\partial}{\partial t}\Psi, \tag{6}$$

and the time-independent version in Eq. (5) reads

$$-\frac{\hbar^2}{2m}\frac{\partial^2}{\partial x^2}\psi_n = E_n\psi_n \tag{7}$$

inside the box given our potential in Eq. (2). [1]

2.2. Dimensionless variables

We now have the equations needed to solve the system, but to do so effectively with numerical simulations we need dimensionless variables for time and space. This is done since number representation on computers do not contain any units. Additionally, dimensionless variables helps scale the problem to a convenient range for numbers on a computer, which improves numerical stability. The new dimensionless variables for time and space becomes $t' = t/t_0$ and $x' = x/x_0$. Since our potential has a well-defined width L, choosing $x_0 = L$ gives $x' \in [0, 1]$. We thus set the characteristic length to the length of the system and the spacial parameter can be interpreted as the fraction of the total length of the system. This is also a suitable range for numerics and is easily compared to different experiments.

Our equations can thus be transformed to use dimensionless variables, with the new derivatives being

$$\frac{\partial\Psi(x', t')}{\partial t} = \frac{\partial\Psi(x', t')}{\partial t'}\frac{\partial t'}{\partial t} = \frac{\partial\Psi(x', t')}{\partial t'}\frac{1}{t_0} \tag{8}$$

and

$$\frac{\partial^2\Psi(x', t')}{\partial x^2} = \frac{\partial}{\partial x}\left(\frac{\partial\Psi}{\partial x'}\frac{\partial x'}{\partial x}\right) = \frac{1}{L^2}\frac{\partial\Psi(x', t')}{\partial x'^2}, \tag{9}$$

where the last equality uses $\partial x'/\partial x = 1/x_0$ with $x_0 = L$. If we insert these derivatives into the time-dependent Schrödinger equation (6) we get

$$i\frac{\partial\Psi(x',t')}{\partial t'}\frac{1}{t_0} = -\frac{\hbar}{2mL^2}\frac{\partial^2\Psi(x',t')}{\partial x'^2} \tag{10}$$

which is

$$i\frac{\partial\Psi}{\partial t'} = -\frac{\partial^2\Psi}{\partial x'^2} \tag{11}$$

when $t_0 = 2mL^2/\hbar$. The same approach can be used for the time-independent Schrödinger equation (5) giving

$$-\frac{\partial^2\psi_n}{\partial x'^2} = \frac{2mL^2}{\hbar^2}E_n\psi_n = \lambda_n\psi_n. \tag{12}$$

Eq. (12) has the relation between the eigenvalues λ_n and the energy E_n given by $\lambda_n = 2mL^2/\hbar^2 E_n = t_0 E_n/\hbar$. In total, the dimensionless variables read

$$x' = \frac{x}{L}, \quad t' = \frac{\hbar}{2mL^2}t, \quad \lambda_n = \frac{2mL^2}{\hbar^2}E_n, \tag{13}$$

with $x_0 = L$ and $t_0 = 2mL^2/\hbar$.

2.3. Boundary conditions

The probability density for the particle is $|\Psi(x,t)|^2$ and since the box potential given by eq. (2) has infinitely high walls, the particle has zero probability at being inside the walls. This gives the boundary condition $|\Psi(x,t)|^2 = 0$ at the walls when $x \in \{0, L\}$. For the dimensionless variables x' and t' the boundary conditions follow the same reasoning and thus $|\Psi(x,t)|^2 = 0$ at the walls when $x' \in \{0, 1\}$.

These boundary conditions can be applied to Eq. (12) which has the general solution $\psi_n(x') = C\sin(kx') + D\cos(kx')$. The left boundary $\psi_n(0) = 0$ dictates that $D = 0$, and the right boundary $\psi_n(1) = C\sin(k) = 0$ for the non-trivial case when $C \neq 0$ gives $k = n\pi$ for $n = 1, 2, ...$ We thus have the equation $\psi_n(x') = C\sin(n\pi x')$ which should be properly normalized by $\int_0^1 |\psi_n(x')|^2 dx' = 1$ in which case $C = \sqrt{2}$. The exact and normalized solution to Eq. (12) is then

$$\psi_n(x') = \sqrt{2}\sin(n\pi x') \tag{14}$$

for $n = 1, 2, 3, ...$ The solution in Eq. (14) can then be inserted into Eq. (12)

$$-\frac{\partial^2\psi_n(x')}{\partial x'^2} = (n\pi)^2\sqrt{2}\sin(n\pi x') = (n\pi)^2\psi_n(x'), \tag{15}$$

which gives the eigenvalues $\lambda_n = (n\pi)^2$.

2.4. Eigenfunctions

The initial condition Ψ_0 can be expanded in the basis of the eigenfunctions ψ_n, $\Psi_0(x) = \sum_n \alpha_n\psi_n(x)$, which then can be applied to the time evolution of the system in Eq. (4),

$$\Psi(x,t) = \sum_n \alpha_n \exp\left(-\frac{iE_n t}{\hbar}\right)\psi_n(x), \tag{16}$$

and we thus have the time evolution of the system expanded in the eigenfunctions. [1] Applying the dimensionless variables from Eq. (13), Eq. (16) becomes

$$\begin{aligned}\Psi(x',t') &= \sum_n \alpha_n \exp\left(-\frac{iE_n}{\hbar}\frac{2mL^2}{\hbar}t'\right)\psi_n(x') \\ &= \sum_n \alpha_n \exp(-i\lambda_n t')\psi_n(x'),\end{aligned} \tag{17}$$

which gives us the state of the system $\Psi(x',t')$ at any time t'. However, to reach the solution we first need to find the expansion coefficients α_n for the initial condition $\Psi_0(x)$ in the basis of the eigenstates ψ_n. Since eigenstates with different eigenvalues are orthogonal, the coefficients can be found by taking the inner product between the initial state and the eigenstates [1],

$$\alpha_n = \langle\psi_n, \Psi_0\rangle = \int \psi_n^*(x')\Psi_0(x')dx'. \tag{18}$$

2.5. Box with potential barrier

A different type of potential is the infinite well with a finite valued potential barrier inside with strength V_0. This potential is given by

$$V(x) = \begin{cases} 0, & \text{for } 0 < x < \frac{L}{3} \\ V_0, & \text{for } \frac{L}{3} < x < \frac{2L}{3} \\ 0, & \text{for } \frac{2L}{3} < x < L \\ \infty, & \text{otherwise.} \end{cases} \tag{19}$$

The dimensionless (using Eq. (13)) Schrödinger equation is then

$$i\frac{\partial\Psi}{\partial t'}(x',t') = \left(-\frac{\partial^2}{\partial x'^2} + \nu(x')\right)\Psi(x',t'), \tag{20}$$

where $\nu(x') = t_0 V(x)/\hbar$ and the dimensionless barrier strength is $\nu_0 = t_0 V_0/\hbar$. Similarly to Eq. (12) where the potential is set to zero, we get the time-independent Schrödinger equation

$$\left(-\frac{\partial^2}{\partial x'^2} + \nu(x')\right)\psi_n(x') = \lambda_n\psi_n(x'). \tag{21}$$

For a minimum height ν_0 there will be eigenstates ψ_n with energies less than the barrier. These eigenstates with energies $0 < \lambda < \nu_0$ are given by

$$\begin{aligned}f(\lambda) =& e^{\kappa/3}\left(\kappa\sin\left(\frac{k}{3}\right) + k\cos\left(\frac{k}{3}\right)\right)^2 \\ &- e^{-\kappa/3}\left(\kappa\sin\left(\frac{k}{3}\right) - k\cos\left(\frac{k}{3}\right)\right)^2 = 0,\end{aligned} \tag{22}$$

where $k = \sqrt{\lambda}$ and $\kappa = \sqrt{\nu_0 - \lambda}$. [1]

2.6. Numerical solutions

To discretize the time the time-independent Schrödinger equation, we can apply the central difference approximation to the Hamiltonian. The central difference approximation reads

$$F''(x_k) = \frac{1}{(\Delta x)^2}(f_{k+1} - 2f_k + f_{k-1}) + O((\Delta x)^2), \tag{23}$$

and when applied to Eq. (21) we get

$$-\frac{1}{(\Delta x')^2}(\psi_{n,k+1} - 2\psi_{n,k} + \psi_{n,k-1}) + \nu_k\psi_{n,k} = \lambda_n\psi_{n,k}, \tag{24}$$

where k indicates the index of the discretized x' when it's discretized into N steps. In matrix form Eq. (24) is $\mathbf{A}\vec{\psi}_n = \lambda_n\vec{\psi}_n$, where $\mathbf{A}$ is a $N\times N$ tridiagonal matrix with $2/(\Delta x')^2+\nu_k$ on the diagonal and $-1/(\Delta x')^2$ on the off-diagonals. In the case where the barrier strength $\nu_0 = 0$ the equation reduces to Eq. (12). An alternative solution to the time evolution of the Schrödinger equation not based on the eigenstates is step-by-step methods. One such method is the forward Euler method which we get by approximating the exponential in Eq. (4) with $\exp(-i\Delta t'\hat{H}') \approx 1 - i\Delta t'\hat{H}'$ and thus we get an equation for one step,

$$\Psi(x', t' + \Delta t') = \left(1 - i\Delta t'\hat{H}'\right)\Psi(x', t'). \tag{25}$$

However, this method does not preserve the probabilities in the Schrödinger equation. Choosing a unitary approximation of the exponential will preserve the probabilities. This gives a Crank-Nicolson scheme which reads [1]

$$\left(1 + \frac{i}{2}\Delta t'\hat{H}'\right)\Psi(x', t' + \Delta t') = \left(1 - \frac{i}{2}\Delta t'\hat{H}'\right)\Psi(x', t'). \tag{26}$$

2.7. Rabi oscillations

Eq. (27) presents a new time-dependent potential,

$$V(x) = \begin{cases} 0, & \text{for } 0 < x < \frac{L}{3} \\ V_0 & \text{for } \frac{L}{3} < x < \frac{2L}{3} \\ V_r(t) & \text{for } \frac{2L}{3} < x < L \\ \infty, & \text{otherwise.} \end{cases} \tag{27}$$

This system can be described as an effective two-level with tunneling amplitude

$$\tau = \int_0^L dx'\psi_0(x')\left(-\frac{\partial^2}{\partial x'^2} + \nu(x', \nu_r)\right)\psi_1(x') \tag{28}$$

between the two states. We can enforce a population transfer between the two states, so-called Rabi oscillations, end we end up with the time evolution equation

$$\left(1 + i\Delta t'(2\hbar)^{-1}\hat{H}_{1I,k}\right) f_k = f_0 + \sum_{i=1}^{k-1}\left(-i\Delta t'\hbar^{-1}\right)\hat{H}_{1I,i}f_i, \tag{29}$$

where f represents the discretized wave function ψ. The probability that this system is in state $|g_0\rangle$ after time t' is $p(t') = |\langle g_0|\psi(t')\rangle_I|^2$, and has the analytical solution $p(t') = \sin^2(t'\tau/2\hbar)$. [1]

3. Numerical implementation

The code used to model these equations is written in Python, mainly with the NumPy and SciPy libraries. For the integration, the trapezoidal rule was used with the NumPy function *trapz*.

4. Results

4.1. Particle confined in box

The eigenvalues for the expression in Eq. (12) is plotted together with the analytical solution in Eq. (14) in Figure 1. For the corresponding eigenfunctions for both the numerical and analytical case, the root-mean-square deviation (RMSE) between the two is plotted in Figure 2 for different step lengths Δx. The orthogonality of the numerically computed eigenstates were validated by the integral in Eq. (18), and all coefficients had values below $10^{-}9$.

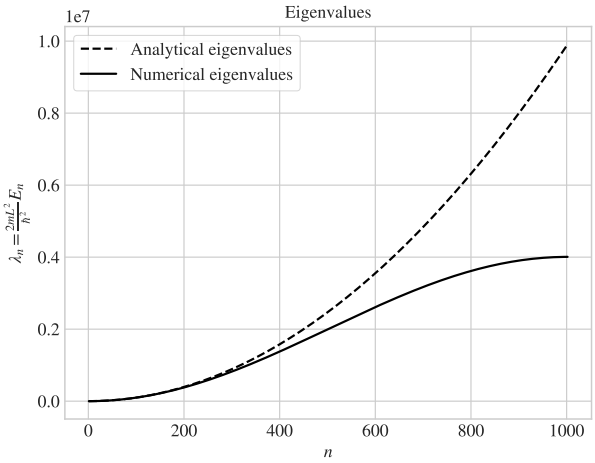

Figure 1. *Numerical and analytical eigenvalues for single particle in box as a function of eigenstates n.*

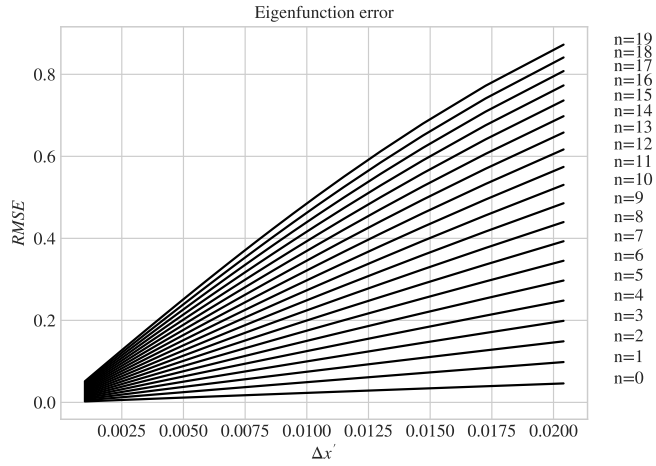

Figure 2. *Root-mean-square deviation for the numerical and analytical eigenfunctions for single particle in box as a function of step length $\Delta x'$, for eigenstates n.*

The time evolution of $\Psi(x', t')$ is found with Eq. (17). Figure 3 shows the time evolution when the initial wave function is the first analytical eigenfunction (Eq. (4) with $n = 1$), and Figure 4 when the initial condition is the delta function $\Psi_0(x') = \delta(x' - 1/2)$.

4.2. Box with potential barrier

For the box potential in Eq. (19), the wave eigenvalues and eigenstates is the same as when the barrier strength ν_0 is set to zero, matching the results for a normal box. With the potential barrier strength is $\nu_0 = 10^3$ the first eigenvectors and eigenvalues of the system is plotted accordingly in Figure 5.

Setting the initial condition to the superposition between the first two eigenstates $\Psi_0 = (\psi_1 + \psi_2)/\sqrt{2}$ and evolving the

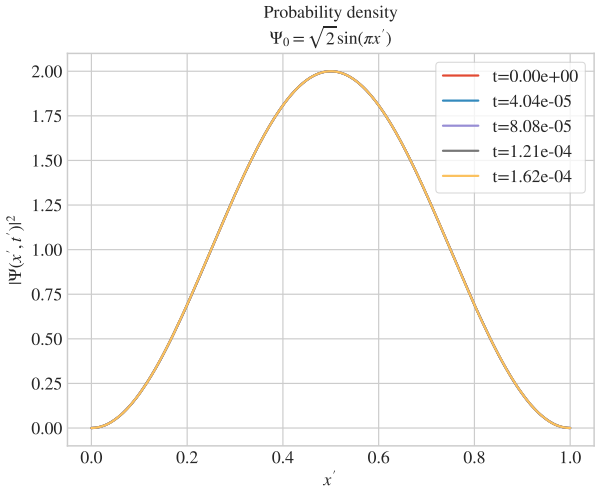

Figure 3. *Time evolution of the probability density of the wave function.*

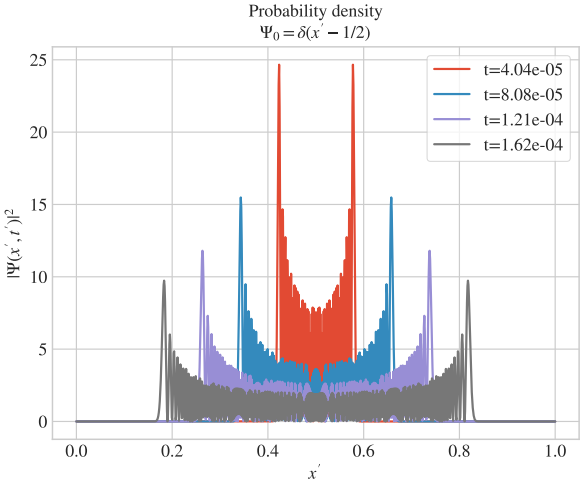

Figure 4. *Time evolution of the probability density of the wave function.*

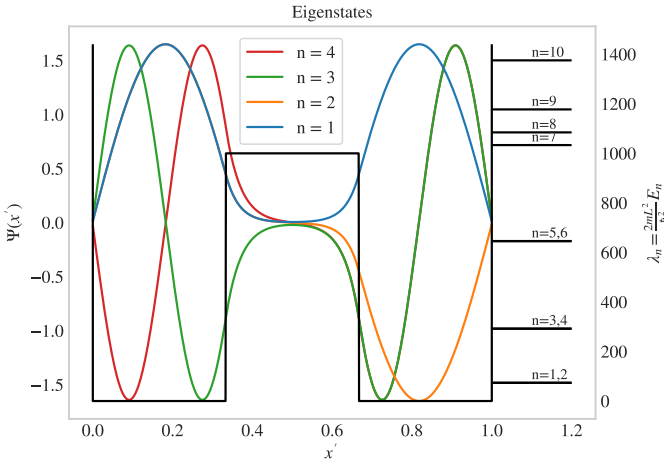

Figure 5. *First four eigenstates of the wave function in a box with potential barrier. On the right is the first ten eigenvalues of the wave function. The black line is the box potential with correct energy strength.*

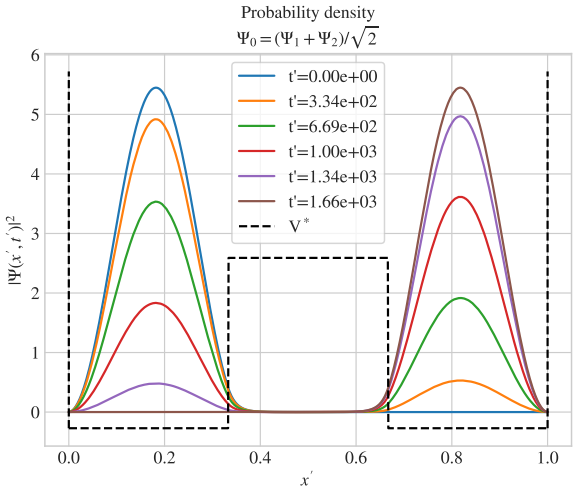

Figure 6. *Probability density of the wave function over time for the given initial condition. The potential V^* has the shape of the correct potential.*

system to time $t' = \pi/(\lambda_2 - \lambda_1)$ with Eq. (17) and Eq. (18) is represented in Figure 6.

The roots of these eigenfunctions can be found with Eq. 22 which in Figure 7 is plotted together with the first six numerically obtained eigenvalues. The number of eigenvalues less than the barrier height is plotted in Figure 8 as a function of barrier strength ν_0. The estimated value of the barrier strength as it goes from one eigenvalue less than ν_0 to no eigenvalues is $\nu_0 = 22.09606$.

The eigenvalues of Eq. (22) was compared to the numerically obtained values in Figure 5 and presented in Table 1.

4.3. Step-by-step schemes

The numerical stability of the Forward Euler scheme in Eq. (25) with the first eigenstate as the initial condition which should remain stationary. This is plotted for different Courant-Friedrichs-Lewy (CFL) numbers, $\Delta t'/\Delta x'$, in Figure 9.

The Crank-Nicolson scheme in Eq. (10) were applied to the initial condition $\Psi_0 = \delta(x' - 1/2)$ and the time evolution is plotted in Figure 10.

4.4. Rabi oscillations

The two lowest eigenvalues for the potential in Eq. (27) is plotted as a function of the barrier strength ν_r in Figure 11, when the middle barrier strength is $\nu_0 = 100$. The corresponding tunneling amplitude τ from the ground state to the excited state in the two level system from Eq. (29) is also plotted. A linear regression of τ was performed and the resulting function became $\tau(\nu_r) = -0.4295\nu_r$.

5. Discussion

5.1. Particle in box

Figure 1 shows that the numerically obtained eigenvalues follows the analytically obtained eigenvalues for the first 200 eigenstates and then starts to flatten out, away from the analytical values. We can thus see that the method which uses expansions in eigenfunctions might give imprecise values when higher eigenstates are considered. This result is also suported by Figure 2 which shows that the root-mean-square (RMSE) deviation between the numerical and analytical eigenfunctions

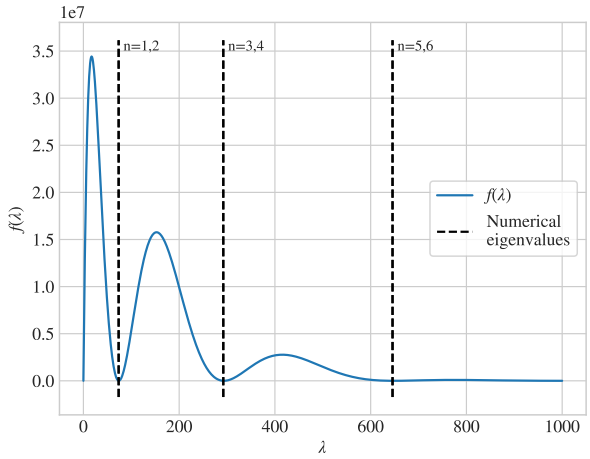

Figure 7. *Analytical roots $f(\lambda) = 0$ plotted together with numerically obtained eigenvalues as vertical lines, where n is the eigenstate.*

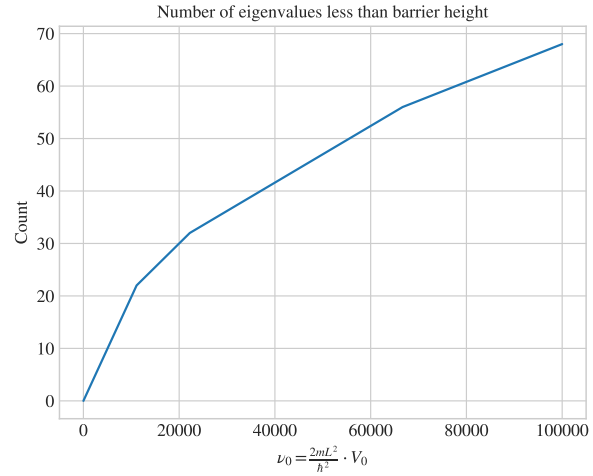

Figure 8. *Number of eigenvalues with energy lower than the barrier strength ν_0 as a function of the barrier strength.*

increase faster for higher eigenstates. The RMSE increases linearly with the step-size ($\Delta x'$), and should thus also be considered when choosing the parameters of the model. A smaller step-size gives less error, but on the other hand the computational expensiveness increases. These results point to that this method works best for smoother initial functions.

When using the expansion method with a smooth initial function such as the first eigenstate, Figure 3 shows that the wave function remains stationary over time, which is the expected case. If the numerical method showed deviations from the stationary state, then this would mean that the method was not stable. In the event of a discontinuous initial wave function such as the delta function, Figure 4 shows that the time evolution gives massive oscillation after time and the wave function disperses away from the center. In this case the numerical method seems to be unstable and does not give the correct results. This might be due to the trapezoidal integration method of the integral in Eq. (18) which does not integrate the delta function properly. A better method would take this into consideration and split up the integral at the discontinuity.

n	**Analytical λ_n**	**Numerical λ_n**	Difference
1	73.598	73.936	0.337
2	73.601	73.938	0.337
3	292.168	293.492	1.324
4	292.191	293.516	1.325
5	645.450	648.264	2.814
6	645.920	648.750	2.830

Table 1. *Analytically and numerically obtained eigenvalues for different eigenstates n.*

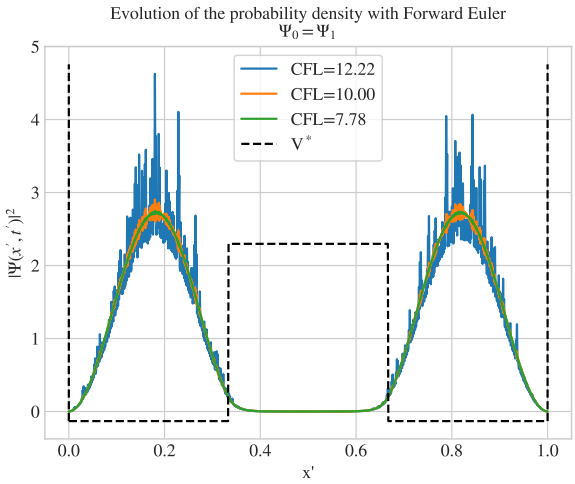

Figure 9. *Time evolution with the Forward Euler scheme for the same time t', for different CFL numbers.*

5.2. Box with potential barrier

The particle in box with potential barrier gives the same results as the method for no potential, when the barrier potential is set to zero. The first four eigenstates of the system with barrier strength 10^3 is shown in Figure 5. We can see that the first two eigenstates are equal on the left side of the barrier and on the right side they are symmetric across the x-axis. The same goes for the 3rd and 4th eigenstates as well. These "pairs" of states should have approximately the same energy, which we can see in Figure 5. As long as the eigenvalues are lower than the potential barrier, we see that the eigenvalues are almost the same for pairs of two. The time-evolution of the probability density of the wave function with the superposition of the two first eigenstates as initial condition is shown in Figure 6. The probability density tunnels the barrier over to the right side, and after time $t' = \pi/(\lambda_2 - \lambda_1)$ the wave function is completely on the other side. This happens because the wave function is not zero inside the finite strength potential barrier and the probability can thus tunnel the barrier.

The eigenvalues of the system with a potential barrier can also be found by Eq. (22). This function is plotted in Figure 7 together with the numerically estimated eigenvalues as vertical lines. We see that the numerically estimated values has approximately the same values as the minimas of the function, which is expected. The roots of this function were estimated and compared to the numerical eigenvalues in Table 1. The values are close and the difference increases with the quantum number. The roots of the function is closer to each other for the "pairs" of energy states, than for the numerical case.

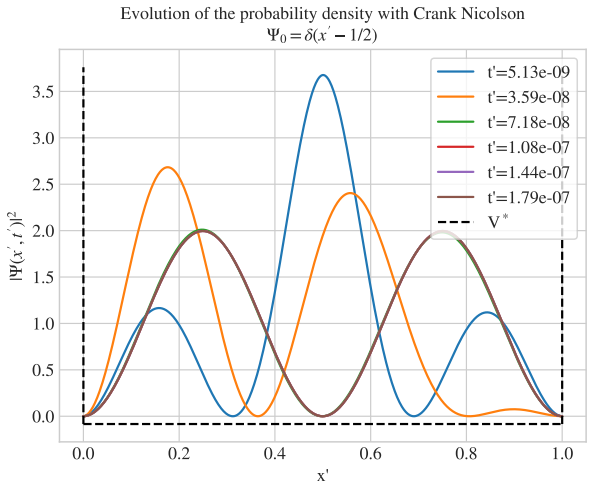

Figure 10. *Time evolution with the Crank-Nicolson scheme for the delta value as initial condition.*

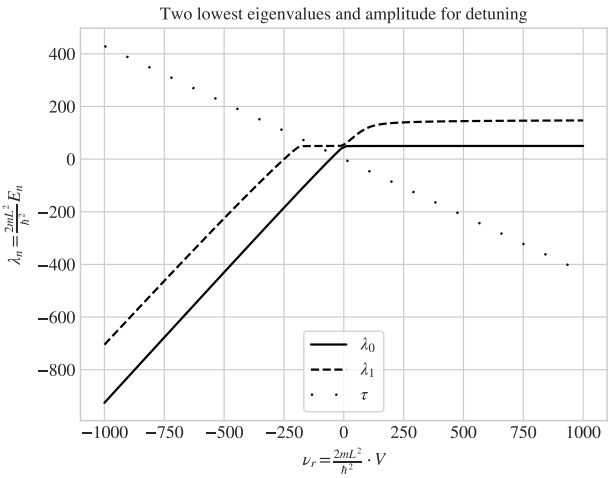

Figure 11. *The two first eigenvalues of the system as a function of the barrier height ν_r.*

The number of eigenvalues less than the barrier strength are plotted in Figure 8 and we can see that there is a shift between zero and one value. This threshold strength were after more precise calculations estimated to be $\nu_0 = 22.09606$.

5.3. Step-by-step methods

The time evolution of the wave function can also be solved with the Forward Euler scheme. It is known that many numerical step-methods are highly dependent on the parameters for stability. One such number is the CFL number, $\Delta t'/\Delta x'^2$. The probability density of the first eigenstate is evolved with the Euler scheme to the same time point with three different CFL number in Figure 9. This state should remain stationary but we see that for CFL number 10 and above, there occurs numerical instabilities and the wave function starts to move away from the true solution. This does not seem to happen at CFL = 7.78, and the threshold for instabilities might thus be 10.

The method to evolve the Schrödinger equation with expansion in the eigenstates might be incorrect in cases with discontinuities and very steep slopes, as this is hard to represent numerically in the basis of a finite number of eigenstates. The Crank-Nicolson method might deal with such cases more effectively, which was tested with the delta initial function for zero barrier strength in Figure 10 to compare to the solution in Figure 4. We can see that the time evolution is solved without the same noisy oscillations as in the expansion case. Additionally, the wave function in the Crank-Nicolson method seems to equilibrate in one state and stay there. The Crank-Nicolson scheme thus performs better for initial conditions with abrupt changes.

5.4. Rabi oscillations

For the barrier with periodic detuning, the two lowest eigenvalues are plotted in Figure 11. The two eigenvalues mostly increase linearly for negative ν_r and plateaus for positive values . This makes sense because when the barrier strength ν_r is larger than ν_0 not much tunneling will happen. We can also notice that the eigenvalues are closest at $\nu_r = 0$, which corresponds to the previously investigated potential where the two first eigenvalues were very close in value. The tunneling amplitude from the ground state to the excited state can also be seen to decrease linearly with ν_r.

6. Conclusion

The error in eigenvalues for the method that uses expansion in eigenstates, increases with increasing quantum number, however, for the first few states and small enough spatial step-size the error is low. This method performs well for smooth initial functions, but struggles with numerical instabilities with functions that has very steep slopes or are discontinuous.

Adding a potential barrier in the middle of the box creates eigenstate "pairs" that have symmetric eigenfunctions and very close eigenvalues. This only happens for states with energy below the potential barrier. The time evolution of the probability density for one such state is found to tunnel through the barrier, clearly showing the quantum physical phenomena. The eigenvalues lower than the barrier strength were also found by an analytical equation minimized with a numerical function. The resulting eigenvalues corresponded to those found earlier. Additionally, the number of eigenstates with energy lower than the potential barrier were investigated and it was found that the threshold to have one or more eigenvalues under the barrier were for the barrier strength $\nu_0 = 22.09606$.

The forward Euler step method were used to evolve the wave function in time, and it was found that it has a strong dependence on the CFL number, where a number of 10 or higher makes the method numerically stable. Where the method of expanding in the eigenstates were found to be unstable, the Crank-Nicolson scheme performed better.

The detuned two state system gave more insight into tunneling. For increasing potential ν_r the tunneling amplitude decreased linearly. Eigenvalues of the system were closest when $\nu_r = 0$, thus comparable to the box potential with only one barrier, where the system had "pairs" of eigenvalues.

References

[1] J. Kjellstadli, A. Sala, and I. Simonsen, “Assignment 2: The world of quantum mechanics”, Spring 2024.